Original Article

Preclinical Xenograft Models of Human Sarcoma Show Nonrandom Loss of Aberrations

Stine H. Kresse, PhD[1]; Leonardo A. Meza-Zepeda, PhD[1,2]; Isidro Machado, MD[3]; Antonio Llombart-Bosch, MD[3]; and Ola Myklebost, PhD[1,2]

BACKGROUND: Human tumors transplanted into immunodeficient mice (xenografts) are good preclinical models, and it is important to identify possible systematic changes during establishment and passaging in mice. **METHODS:** High-resolution microarray-based comparative genomic hybridization (array CGH) was used to investigate how well a series of sarcoma xenografts, including 9 patient/xenograft pairs and 8 early versus late xenograft passage pairs, represented the patient tumor from which they originated. **RESULTS:** In all analyses, the xenografts were more similar to their tumor of origin than other xenografts of the same type. Most changes in aberration patterns were toward a more normal genome complement, and the increased aberrations observed were mostly toward more loss. In general, the changes were scattered over the genome, but some changes were significant in osteosarcomas. These were rather focused and consistent with amplifications frequent in patient samples, involving the genes platelet-derived growth factor receptor A (*PDGFRA*), cysteine-rich hydrophobic domain 2 (*CHIC2*), FIP-like 1 (*FIP1L1*), ligand of numb-protein X1 (*LNX1*), RAS-like family 11 member B (*RASL11B*), and sec1 family domain containing 2 (*SCFD2*), probably a sign of continued tumor progression. Some changes that disappeared may have been involved in host-stroma interactions or chemotherapy resistance, possibly because of the absence of selection in the mouse. **CONCLUSIONS:** Direct xenografts reflected well the genomic patterns of their tumors of origin. The few significant aberrations that were lost during passaging in immune-defective mice may have been caused by the lack of selection in the new host, whereas aberrations that were gained appeared to be the result of general tumor progression rather than model-specific artifacts. ***Cancer*** **2012;118:558–70.** © *2011 American Cancer Society.*

KEYWORDS: microarray-based comparative genomic hybridization, chromosomal aberration, sarcoma, nude mouse, xenograft.

Pieces of human malignant tumors can be implanted into immunodeficient mice, where they may grow as xenografts supported by murine stroma, blood supply, etc.[1] However, transplantations frequently fail, in particular for low-grade tumors; and xenografts may be established preferentially from more aggressive tumors[2] and, thus, may not reflect the whole spectrum of human malignancies. Once established, xenograft lines may be grown indefinitely as heterogeneous tissue better resembling the original tumors than cell lines grown in vitro. Such direct xenografts, or "tumorgrafts," are very useful as cancer models for preclinical experiments,[3-5] although many properties may not correctly represent the original tumors (eg, level of circulation, extent of hypoxia, slowly growing regions, reactions to altered levels of hormones and metabolites, and interactions with stroma and the immune system). A xenograft is established from a small piece of tissue, usually a few cubic millimeters, and may not represent well other tumor parts or even the majority of the tumor, although intratumoral heterogeneity may be maintained.[6] Furthermore, the selection pressures may differ in a mouse host, and new gene aberrations may appear upon establishment and passaging.

Corresponding author: Prof. Ola Myklebost, Department of Tumor Biology, The Norwegian Radium Hospital, Oslo University Hospital, N-0310 Oslo, Norway; Fax: 0047-22781795; ola.myklebost@imbv.uio.no

[1]Department of Tumor Biology, The Norwegian Radium Hospital, Oslo University Hospital, Oslo, Norway; [2]Norwegian Microarray Consortium, Department of Molecular Biosciences, University of Oslo, Oslo, Norway; [3]Department of Pathology, University of Valencia, Valencia, Spain

We are grateful to Alexandr Kristian and colleagues at the Animal facility and Ståle Nygård at the Bioinformatics facility for assistance with the animal work and statistics, respectively.

DOI: 10.1002/cncr.26276, **Received:** February 1, 2011; **Revised:** April 7, 2011; **Accepted:** April 21, 2011, **Published online** June 28, 2011 in Wiley Online Library (wileyonlinelibrary.com)

Xenografts also may be established indirectly by the injection of in vitro cell lines into mice. However, such cell lines are less useful as preclinical models,[7] because specific mutations may be induced during in vitro culture,[8] their expression program may be irreversibly changed,[9] and their response to therapy frequently differs from that of the patients.[7] Also, mouse allografts seem to be less useful for preclinical purposes.[7]

It is important to know how similar xenografts are to their tumor of origin and how faithfully their genomes are maintained upon passaging in a xenobiotic host. Even when a cancer cell well represents its tumor of origin, patterns of gene expression and signaling are dynamic and will be influenced by the growth pattern, vascularization, interaction, and signaling with host stroma cells and by the reduced or absent interactions with the immune system. Still, it has been demonstrated that expression profiles of nonmatched sarcoma xenografts cluster together with patient samples of the same tumor type, suggesting good overall representation of the relevant phenotypes, although minor but critical features may be altered.[10,11] However, those analyses focused on overall similarity rather than detecting differences, which was our focus in the current study.

Chromosomal copy number profiles are less dynamic than expression profiles, and it is reasonable to expect that aberrations represented in the cancer cells that contribute to the xenograft are maintained during establishment. If there is a strong new selection pressure for growth in the xenogeneic host, new aberrations may appear as soon as in the first passage. Such changes should be recurrent, whereas more random changes would be caused by sampling effects. Therefore, our objective was to investigate how faithfully chromosomal copy number aberrations are maintained during the establishment and passaging of xenografted human tumors into immunodeficient mice. Sarcomas may have different global patterns of chromosomal aberrations, extending from largely normal karyotypes that contain specific translocations or complex marker chromosomes to the very unstable and complex karyotypes of osteosarcomas.[12] Therefore, we investigated xenografts that represented both chromosomally stable and unstable sarcoma types.[12]

This study is part of a trans-European effort to establish and characterize an extensive set of preclinical models representing important genetic and biologic subtypes of osteosarcoma (see http://www.eurobonet.eu; accessed January 2011). Current European Network to Promote Research into Uncommon Cancers in Adults and Children: Pathology, Biology, and Genetics of Bone Tumors (EuroBoNeT) preclinical models consist of a panel of 19 in vitro osteosarcoma cell lines[13] and an extensive panel of 25 osteosarcoma direct xenografts (Kresse et al, unpublished data). In the current study, we selected several samples, including both osteosarcomas and soft tissue sarcomas, to investigate the fidelity of genomic maintenance through the establishment and passaging of xenografts.

MATERIALS AND METHODS

Tumor Samples and Xenografts

Eleven human sarcomas were selected from a tumor collection in the Department of Tumor Biology at the Norwegian Radium Hospital (Oslo, Norway) and 4 from the Department of Pathology at the University of Valencia (Valencia, Spain). All tumors were diagnosed according to the current World Health Organization classification.[14] Informed consent and sample collection were approved by the Ethical Committee of Southern Norway (Project S-06132) and the Institutional Ethical Committee of Valencia University. Clinical samples were collected immediately after surgery, cut into small pieces, and either implanted as described below or frozen in liquid nitrogen and stored at −70°C until use. In total, 36 samples, including patient samples and xenografts, were analyzed. Clinical data for the patient samples are provided in Table 1.

Athymic, "nude" mice (Balb/c: nu/nu) were either bred in the animal facility and weaned after 21 days (Oslo samples) or purchased from Iffa-Credo (Lyon, France; Valencia samples) and were maintained in a pathogen-free environment at controlled temperature (21 ± 0.5°C) and humidity (55%-65%) on a 12-hour light cycle. All procedures involving animals were performed according to protocols approved by the Animal Care and Use Committee at the hospital and in compliance with the National Ethics Committee's guidelines on animal welfare and the council directive of the European Communities on the protection of animals used for experimental and other scientific purposes. One to 2 mm^3 of fresh tumor tissue were implanted subcutaneously in the flanks of nude mice and propagated by serial transplantation.[15]

Microarray-Based Comparative Genomic Hybridization

The genomic microarray that we used contained 4549 bacterial artificial chromosome (BAC) clones and P1 artificial chromosome (PAC) clones representing the human genome at approximately 1 Mb resolution as well as the

Table 1. Clinical Data for Tumor Samples

Sample	Sample Origin	Patient Age, y	Sex	Diagnosis	Subtype	Grade[a]	Sample Location	Size, cm[b]	Metastasis, mo[c]	Status	Follow-Up, mo[d]
GIST5	Metastasis	53	Male	GIST	—	High risk	Liver	6	73	DD	101
LS3	Primary	78	Male	LS	Pleo	4	Upper trunk	13	NM	DOC	7
LS28	Primary	68	Male	LS	Mixed type	4	Intra-abdominal	26	MD	DD	10
LS70	Primary	70	Male	LS	Pleo	4	Retroperitoneum	20	MD	DD	1
MFH77	Primary	31	Male	MFH	SC	3	Facial bone	10	41	DD	76
MPNST2	Primary	46	Male	MPNST	—	4	Upper leg	40	MD	DD	1
OS8	Metastasis	16	Male	OS	Obl	4	Lung	11	3	DD	19
OS46	Primary	17	Male	OS	Cho	4	Pelvis	11.5	12	DD	18
OS47	Primary	12	Male	OS	SC/Pleo	4	Humerus	16	NM	NED	74
OS51	Primary	18	Female	OS	Obl/Tel	4	Femur	26.5	MD	DD	22
OS56	Primary	8	Male	OS	Obl/Fbl	4	Humerus	10.5	NM	NED	63
ABDA[e]	Metastasis	27	Female	OS	Obl	4	Pelvis	4.7	NA	DD	14
JAH[e]	Primary	40	Male	OS	Pleo	4	Femur	NA	36	DD	39
JMC[e]	Primary	NA	Male	OS	NA	4	NA	2	NA	NA	NA
SJG[e]	Primary	NA	Male	OS	Obl	4	Humerus	9	NA	NA	NA

Abbreviations: Cho, chondroblastic; DD, dead of disease; DOC, dead of other cause; Fbl, fibroblastic; GIST, gastrointestinal stromal tumor; LMS, leiomyosarcoma; LS, liposarcoma; MD, metastasis at diagnosis; MFH, malignant fibrous histiocytoma; MPNST, malignant peripheral nerve sheath tumor; NA, not available; NED, no evidence of disease; NM, no metastasis; Obl, osteoblastic; OS, osteosarcoma; Pleo, pleomorphic; SC, spindle cell; Tel, telangiectatic.

[a] Grading is based on a 4-tiered system used by the Scandinavian Sarcoma Group. GISTs are graded according to size and mitotic count.

[b] Values indicate the greatest dimension of the tumor.

[c] Values indicate the time from diagnosis to first metastasis.

[d] Values indicate the time from diagnosis to last follow-up.

[e] ABDA, JAH, JMC, and SJG are osteosarcomas.

minimal tiling path between 1q12 and the beginning of 1q25. Detailed information on the construction and preparation of the microarray has been published previously.[16] The microarrays were provided by the Norwegian Microarray Consortium (http://www.microarray.no; accessed January 2011).

Microarray-based comparative genomic hybridization (array CGH) was performed essentially as described previously.[16] In brief, approximately 500 ng of *Dpn*II-digested total genomic DNA was labeled by random priming using BioPrime DNA Labeling System (Invitrogen, Carlsbad, Calif) and indocarbocyanine (Cy3)-deoxycytidine triphosphate (dCTP) (tumor) or indodicarbocyanine (Cy5)-dCTP (reference) (Perkin Elmer, Waltham, Mass). Labeled tumor and reference DNA samples were combined together with 135 μg human Cot-1 DNA (Invitrogen). Hybridization was performed using an automated hybridization station, GeneTAC (Genomic Solutions/Perkin Elmer), and agitating the hybridization solution for 42 to 46 hours at 37°C. The arrays were scanned using an Agilent G2565BA scanner (Agilent Technologies, Santa Clara, Calif), and the images were segmented using GenePix Pro 6.0 (Molecular Devices, Sunnyvale, Calif). Further data processing, including filtering and normalization, was performed using array CGH as described previously.[16,17]

Array CGH Data Analysis

The complete array CGH dataset for the 36 samples analyzed can be viewed in the ArrayExpress microarray database (accession no. E-MEXP-2576; http://www.ebi.ac.uk/arrayexpress; accessed January 2011). Clones belonging to chromosomes 1 through 22 with known unique chromosomal location in Ensembl version 33 (http://www. ensembl.org; accessed September 2005) were considered for analysis (3351 clones). Because of experimental variation in normal control experiments, 22 clones (0.7%) were discarded, as described previously.[16] In addition, clones with missing values in $\geq$11 of the 36 samples were discarded, leaving 3202 clones for analysis. The remaining missing values were imputed with a K-Nearest Neighbor Algorithm normalization using "Significance Analysis of Microarrays."[18]

Clustering of all samples was performed using J-Express Pro (version 2.7; MolMine AS, Bergen, Norway)[19] with average linkage (the weighted pair group method with arithmetic mean) as the cluster method and Pearson correlation as the distance metric. To determine copy number changes, quantile normalized $\log_2$ ratios were segmented using the circular binary segmentation (CBS) algorithm[20] in CGHweb (http://compbio.med.harvard.edu/CGHweb/; accessed January 2011) with an α value of .05. Segmented $\log_2$ ratios >0.25 were scored as gain, and $\log_2$ ratios less than -0.25 were scored as loss. To identify changes in copy numbers between 2 samples, the difference between the segmented $\log_2$ ratios was calculated for each clone. Segments consisting of at least 4 consecutive clones with a $\log_2$ ratio difference of at least ± 0.25 were scored as chromosomal regions with changes in copy number.

To examine whether there were chromosomal segments with enrichment of certain copy number changes, the following statistical test was carried out: Under the null hypothesis that copy number changes are distributed evenly across the genome, the number of changes of the different types within a given chromosomal segment has a multinomial distribution with a probability vector equal to the observed proportions for the different types over the whole genome. On the basis of this distribution, (raw) *P* values were calculated for the observed counts for each chromosomal segment (for patient vs xenograft and early vs late xenograft for both soft tissue tumors and osteosarcomas). The raw *P* values were adjusted for multiple testing using the procedure described by Benjamini and Hochberg.[21]

RESULTS

The chromosomal copy number profiles of sample pairs from 6 soft tissue sarcomas and 9 osteosarcomas, representing 9 patient sample-xenograft pairs and 8 early late xenograft passage pairs, were analyzed using a 1-Mb genomic (BAC/PAC) microarray. Two series contained both a patient sample and more than 1 passage level of the xenograft. Clinical data on the patient samples are listed in Table 1. A complete review of the histologies and an extended set of protein markers were published elsewhere.[22] Overall, the xenografts were more homogeneous and had a higher fraction of proliferating cells than the patient tumors.[22]

Figure 1 is a heat map of the entire dataset after unsupervised clustering of the samples. This heat map indicates that the samples aggregated into 3 main groups, all of which contained both soft tissue sarcomas and bone sarcomas. Thus, there were no overall characteristics of the genomic profiles that clearly distinguished the 2 main types of patient or xenograft samples. Conversely, all xenografts clustered closely with their tumor of origin or the other passage of the same xenograft, as indicated by the lengths of the branches of the dendrogram in Figure 1.

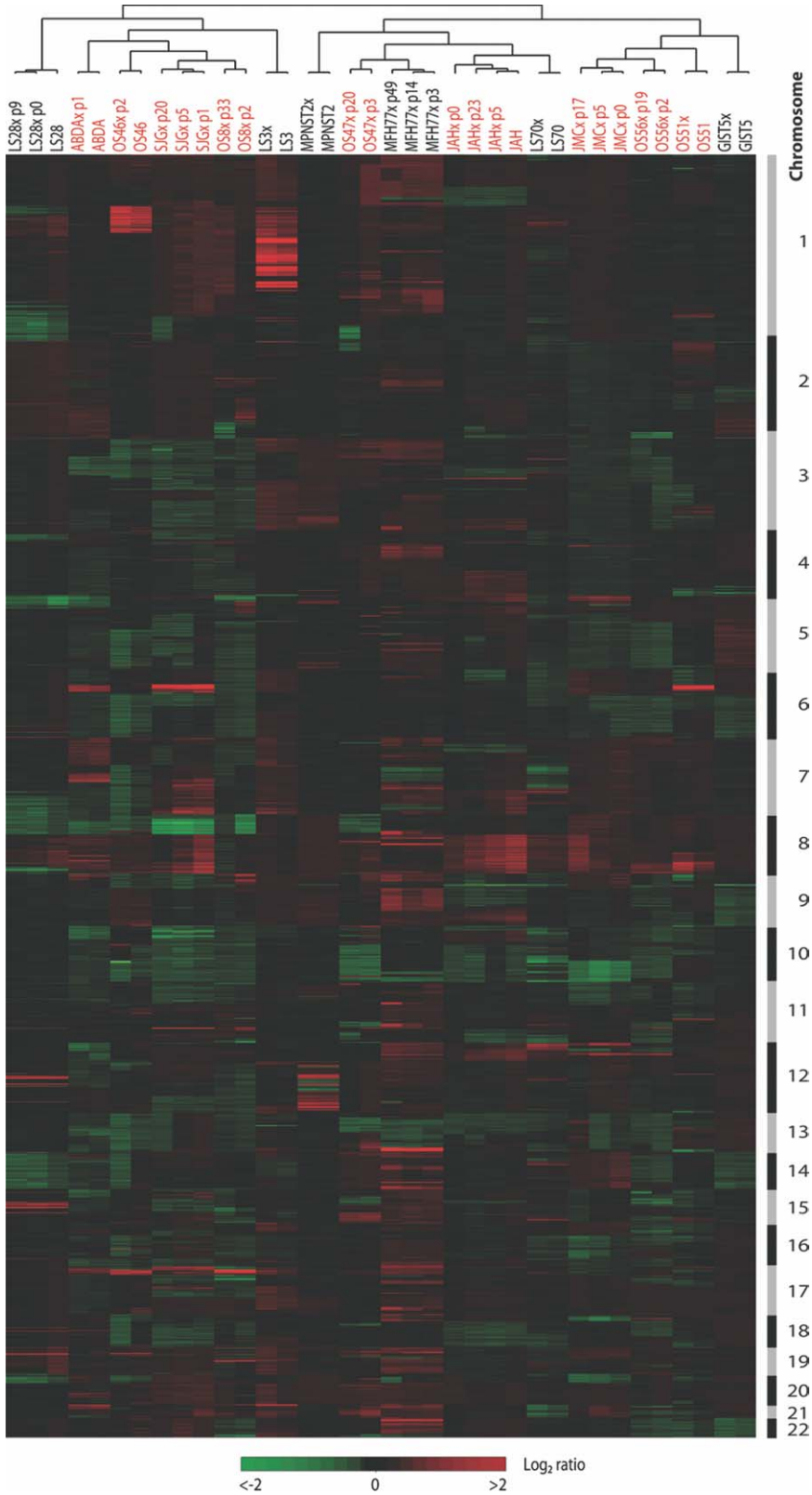

Figure 1. Unsupervised hierarchical clustering of 36 sarcoma samples, including patient tumors and their derived xenografts, using DNA copy number ratios relative to a pool of normal diploid DNA. In total, 3202 unique genomic clones are shown in chromosomal order from the chromosome 1 short arm telomere (1ptel) to the chromosome 22 long arm telomere (22qtel). Chromosomes are indicated by the black-and-gray bar on the right. Soft tissue tumors are indicated on the top in black letters (liposarcoma [LS], malignant peripheral nerve sheath tumor [MPNST], malignant fibrous histiocytoma [MFH], and gastrointestinal stromal tumors [GIST]); and osteosarcomas (OS) are indicated on the top in red letters (including the tumors designated ABDA, SJG, JAH, and JMC). Red areas indicate increased DNA copy number; green areas, decreased DNA copy number.

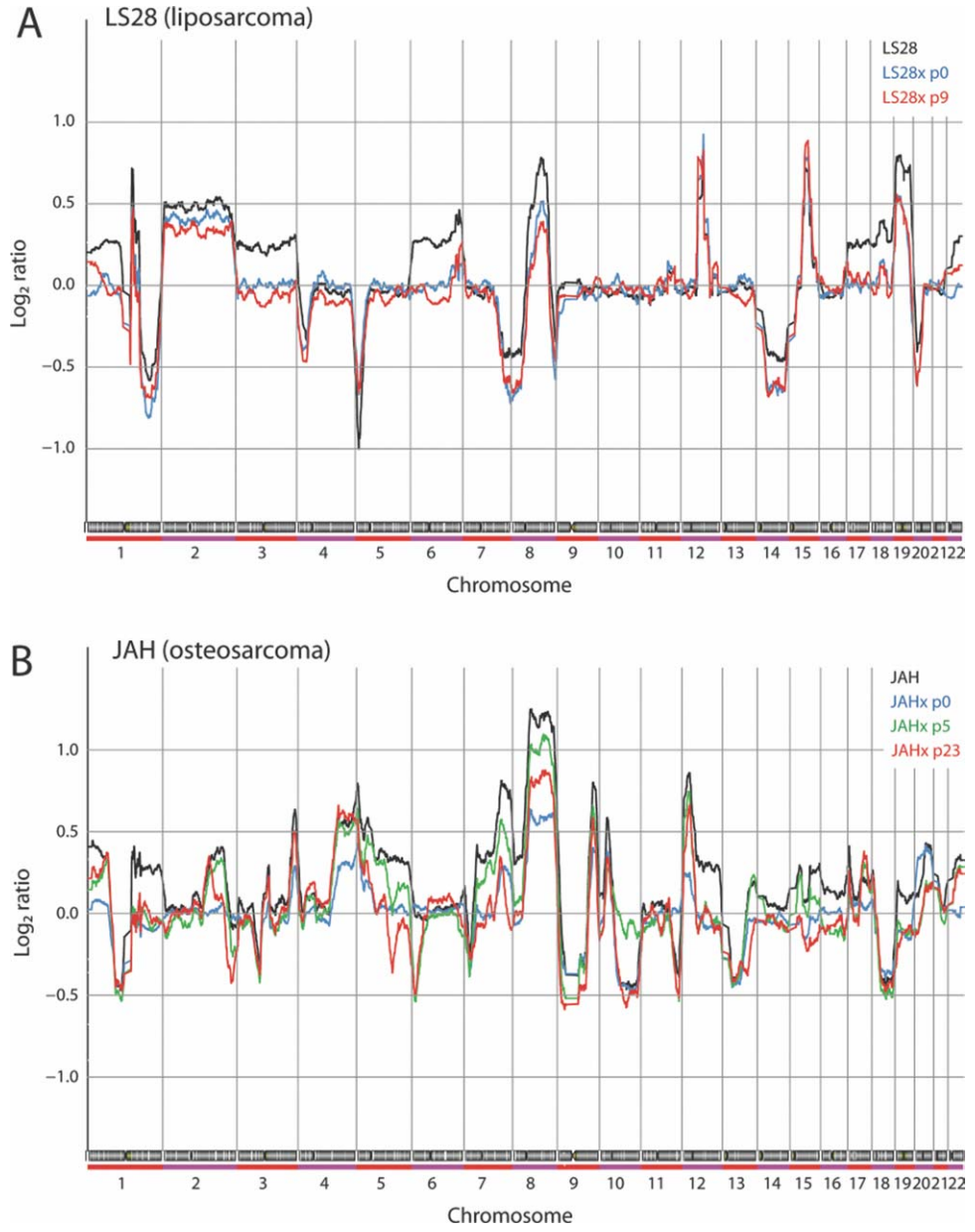

Figure 2. Representative whole-genome chromosomal copy number profiles of a patient tumor and its derived xenografts of different passages are illustrated for (A) a soft tissue sarcoma and (B) an osteosarcoma. The $\log_2$ ratio for each of the genomic clones is plotted according to chromosome position and is smoothed with a moving average of 15 clones.

Samples with the same tumor origin were more similar than any of the different xenografts. Although this indicates a high degree of overall similarity between donor tissues and the resulting xenografts, it does not rule out important changes that may be selected for during establishment and passaging in a foreign host.

Detailed copy number profiles for 2 sample sets are provided in Figure 2, whereas all individual ratio plots for all samples and combined plots for sample sets are provided in Supplemental Figure 1 (http://www.ous-research.no/home/myklebost/SuppData; accessed May 2011). The murine stroma components in the xenografts contribute less to the array signals than the human stroma in patient samples and, thus, may result in increased apparent amplitudes of changes in the xenografts. In addition, there may be considerable genetic drift of the aneuploidy chromosome composition and representation of subclones from the original tumor. These phenomena are

Table 2. Minimal Recurrent Regions Altered Between Patient Tumor and First Xenograft Passage

Cytoband	Copy No. Change	Start Clone	End Clone	Size, Mb	Frequency
1q23.2	Decrease	RP11-190A12	RP11-536C5	0.4	4/9
1q25.1	Decrease	RP1-300A12	RP3-436N22	0.6	3/9
4ptel-p16.1	Decrease	CTC-36P21	RP11-117J13	8.2	3/9
4q34.1-q34.3	Decrease	RP11-140M23	RP11-396I22	7.5	3/9
4q35.3-qtel	Decrease	RP11-91J3	CTC-963K6	2.5	3/9
5q35.3	Decrease	RP11-520O10	RP11-281O15	0.6	3/9
6q25.3	Decrease	RP3-336G18	RP3-366M24	3.9	3/9
6q26-q27	Decrease	RP1-257A15	RP3-470B24	4.9	3/9
7q31.1	Decrease	RP11-5N18	RP5-905M6	3.0	3/9
7q33	Decrease	RP11-371N6	RP11-8P6	2.2	3/9
8q24.3-qtel	Decrease	RP5-1118A7	RP5-1056B24	1.8	3/9
9q33.3-q34.12	Decrease	RP11-101K10	RP11-143H20	6.9	3/9
10q11.22	Increase	RP11-292F22	RP11-541M12	2.2	3/9
12ptel-p13.1	Decrease	RP11-519B13	RP11-4N23	13.5	3/9
16q23.2-q23.3	Decrease	RP11-437L22	RP11-2L4	1.1	3/9
16q24.3-qtel	Decrease	RP4-597G12	CTB-121I4	0.1	3/9
17p13.1	Decrease	RP11-208F13	RP11-401O9	0.8	4/9
19p13.2	Decrease	RP11-492L14	RP11-197O4	3.0	3/9
19p13.2	Decrease	CTC-539A10	CTC-359D24	1.6	3/9

Abbreviations: p, short arm; q, long arm; tel, telomere.

illustrated in Figure 2, in which some profiles of whole chromosomes or chromosome arms are shifted up or down while their detailed shapes are retained, indicating loss or gain of a whole corresponding chromosome (arm); whereas, in other cases, new aberrations clearly appear that may represent original clones increasing their fraction or entirely new aberrations selected for in vivo.

To investigate whether certain copy number changes could be selected during establishment or repeated passaging of human cancer cells in the mouse, aberrations were compared between the paired samples. Basically, 4 types of changes may be detected, increased or reduced loss of segments and increased or reduced gain. Reduced amplitudes of gain or loss would most likely be caused by genetic or clonal drift and could be caused by reduced selection pressures in the mouse. Increased amplitudes, conversely, including new aberrations, may represent continued, increased, or new selection pressures in the xenogeneic host but also may be caused by drift. This would always be expected when comparing xenografts with patient samples, as mentioned above. The only way to distinguish drift or noise from systematic selection during growth in mice would be if the changes were recurrent.

Chromosomal copy number aberrations were identified using the CBS algorithm and a fixed threshold, and the segmented log2 ratios with indicated regions of gain and loss for all samples are provided in Supplemental Table 1 (http://www.ous-research.no/home/myklebost/SuppData; accessed May 2011). To compare paired samples, the difference between the segmented $\log_2$ ratios was calculated, and segments consisting of at least 4 consecutive clones with a $\log_2$ ratio difference of at least ± 0.25 were scored. Data for the comparison between the first xenograft passage and corresponding patient tumor are provided in Supplemental Table 2 and, for the comparison between the last and first xenograft passages, in Supplemental Table 3 (http://www.ous-research.no/home/myklebost/SuppData; accessed May 2011).

To identify possible recurrent copy number aberrations between first xenograft passages and corresponding patient tumors and between last and first xenograft passages, the minimal recurrent regions of copy number changes in at least 30% of the sample pairs were identified. The list of minimal recurrent regions altered between first xenograft passages and corresponding patient tumors is provided in Table 2, and the list for last and first xenograft passages is provided in Table 3. In Figure 3, the minimal recurrent regions of copy number aberrations are plotted as heat maps, giving emphasis to the type of changes that may be caused by selection pressures. The heat maps indicate that most changes were toward a more normal profile, and the changes toward more abnormal profiles were scattered over the genome with little common focus. One region of increased loss in 16q23.2-q23.3 was observed after the establishment of 2 of 4 osteosarcoma xenografts, and 2 regions of increased loss on chromosome 15 were observed during passaging of 3 of 6 osteosarcoma xenografts. However, neither of these was

Table 3. Minimal Recurrent Regions Altered Between First and Last Xenograft Passage

Cytoband	Copy No. Change	Start Clone	End Clone	Size, Mb	Frequency
1p21.1-p13.3	Decrease	RP11-202K23	RP11-28P8	6.1	3/8
1q21.1-q21.2	Decrease	RP11-315I20	RP11-301M17	2.3	3/8
1q21.2	Decrease	RP11-35F14	RP4-790G17	0.2	4/8
1q24.2	Decrease	RP5-1018K9	RP11-212E1	1.1	4/8
1q25.2	Decrease	RP11-247D3	RP3-371M1	0.4	4/8
1q25.2	Decrease	RP11-21M7	RP11-18E13	0.7	3/8
4p14-p13	Increase	RP11-343C9	RP11-227F19	2.0	3/8
4q12	Increase	RP11-157C8	RP11-231C18	1.9	3/8
5q23.1-q23.2	Decrease	RP11-249M12	RP11-14L4	6.7	3/8
5q23.2-q23.3	Decrease	RP11-434D11	CTC-352M6	1.7	3/8
6ptel-p24.1	Decrease	CTB-62I11	RP1-257A7	13.2	4/8
6p21.2-p21.1	Decrease	RP3-350J21	RP11-227E22	5.0	3/8
7q11.23-q21.12	Decrease	RP11-107L23	CTB-60P12	12.2	3/8
7q32.3-q33	Decrease	RP11-329I5	RP11-221G19	3.6	3/8
7q34-qtel	Decrease	RP5-1173P7	CTB-3K23	18.2	3/8
8q11.21-q11.23	Decrease	RP11-350F16	RP11-182E14	6.2	3/8
9p24.3-p21.3	Decrease	RP11-48M17	RP11-11J1	20.4	3/8
9p21.3-p21.1	Decrease	RP11-495L19	RP11-20P5	4.7	3/8
9q21.2	Decrease	RP11-490H9	RP11-336N8	1.2	3/8
11p15.5-p15.2	Decrease	RP11-295K3	RP11-13J19	14.3	3/8
11p14.1-p13	Decrease	RP11-466I1	RP11-115P8	6.7	3/8
12q21.2-q21.31	Decrease	RP11-26L7	RP11-531E6	5.2	3/8
12q24.13-q24.21	Decrease	RP3-363I18	RP11-25E2	2.4	3/8
12q24.23-qtel	Decrease	RP11-385C6	CTC-221K18	15.1	3/8
13q21.33-q32.1	Decrease	RP11-184L18	RP11-74A12	24.3	3/8
15q12-q14	Decrease	RP11-570N16	RP11-3D4	6.8	4/8
15q21.1	Decrease	RP11-151N17	RP11-519G16	1.0	4/8
15q26.3	Decrease	RP11-90E5	RP11-168G16	0.4	3/8
16q11.2	Decrease	RP11-5L1	—	-	3/8
20p12.2-p12.1	Decrease	RP4-742J24	RP5-855L24	2.9	5/8
20p11.23-p11.21	Decrease	RP5-1096J16	RP1-234M6	3.5	5/8
21q22.3-qtel	Decrease	RP11-113F1	CTB-63H24	4.5	4/8
22q13.31-q13.32	Increase	CTA-29F11	CTA-299D3	1.8	3/8

Abbreviations: p, short arm; q, long arm; tel, telomere.

significant given the many random changes observed. The most frequent finding was the loss of amplification in 21q22.23-qtel in 5 of 6 osteosarcoma xenografts during passaging ($P = .037$ after correction for multiple testing); however, findings of clear new gains on chromosome 4 in 2 of 6 osteosarcoma samples (both $P = .021$) and reduced loss of 22q13 sequences in 3 of 6 osteosarcoma samples ($P = .0027$) also were significant, because there were so few of these types of alterations. None of these recurrent changes were observed in soft tissue tumors. Most of these chromosomal regions were large, which made the identification of target genes difficult. The complete gene lists are provided in Supplemental Table 4 (http://www.ous-research.no/home/myklebost/SuppData; accessed May 2011).

DISCUSSION

Cancer cell lines are invaluable tools for experimental preclinical studies both in vitro and in vivo, but they do not completely reflect many important properties of human tumors. One well known example is the National Cancer Institute's NCI60 drug-testing panel,[23] and another initiative has put together a comprehensive panel of pediatric xenografts,[24] although it includes few osteosarcoma lines. We have collected a large panel of osteosarcoma cell lines and xenografts as part of a European network of excellence on bone tumor research (http://www.eurobonet.eu; accessed January 2011) that we have begun to characterize thoroughly by expression and genomic profiling techniques and by scoring several important tumor properties.[13,22] Later, in comparisons with data from our panel of clinical samples, we will identify which models best describe clinically important subsets of bone tumors.

Although the histologies, markers, and expression profiles of osteosarcoma xenografts are relatively conserved during transplantation into mice,[11,22] there also are notable differences that may be caused by altered growth patterns and stroma components. Thus, it will be

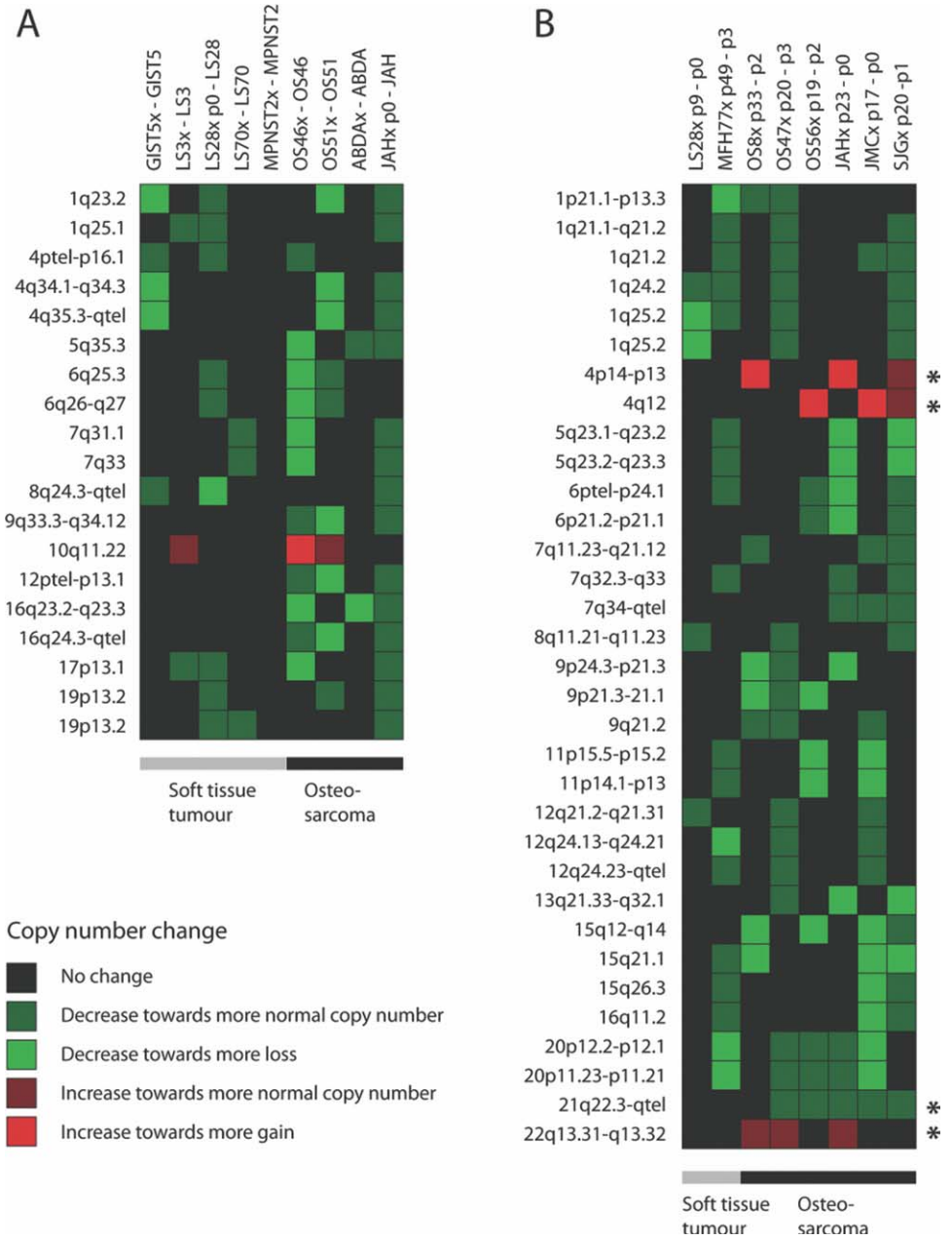

Figure 3. Heat map showing the copy number changes of minimal recurrent regions altered between (A) first xenograft passage and corresponding patient tumor and (B) last and first xenograft passage for all available paired samples. Soft tissue tumors and osteosarcomas are indicated with gray and black bars, respectively. Minimal recurrent regions with a statistically significant copy number change are indicated with an asterisk (*). Red, increases in DNA copy number; green, decreases in DNA copy number.

important to determine whether this reflects altered oncogenic selection pressures that would impact the molecular cancer profiles and, thus, their validity as preclinical models, eg, for drug testing or mechanistic investigations.

To our knowledge, this is the most thorough study to date of its kind. The similarity of glioblastoma xenografts has been compared previously using low-resolution chromosome CGH with nonmatched primary samples and during passaging.[25] Even at such low resolution, some changes were observed during passaging, but only similarity to nonmatched tumors could be determined. In a study of breast cancer xenografts, 1 sample was compared with its tumor of origin, and several changes were

apparent,[2] which also was the case in a study of colon cancer.[6]

How representative the tumor models are depends on several conditions, some of which we have investigated here. One concern is whether the tumors from which we manage to establish cell or xenograft lines represent a cross section of typical cases encountered in the clinic. On the basis of the low number of cases observed here, we could not firmly establish this in the current study, but we will pursue this question by comparing our large EuroBoNeT collection of osteosarcoma xenografts with profiles from clinical samples (Kuijjer et al, unpublished data). However, the over representation of high-grade tumors in the current panel is consistent with the experience that these are the ones more easily established in mice.[2] Although it supposedly is easier to succeed on xenotransplantation to nonobese diabetic/severe combined immunodeficiency (NOD/SCID) recombination gene (rag)-negative mice compared with nude mice, to date, our experience cannot confirm improved grafting in such mice. However, although a panel representative of all tumor stages would be attractive for studies of tumor etiology and progression, the more aggressive tumors represent the most serious clinical challenge and, thus, are the most important, eg, for preclinical drug testing.

The next question is whether the successfully xenotransplanted cancer cells are representative of the tumor of origin. Obviously, there is a sampling effect; implantation of a few cubic millimeters of a large tumor can only give rise to a xenograft originating from some of the implanted cells, which could be from an atypical part of the tumor. However, although the histology may vary significantly across a tumor, it has been demonstrated that both genomic and expression profiles may be more homogeneous.[26] This is supported by the current results, which demonstrate the strong similarity of genomic profiles of the xenografts and their tumors of origin, although the patient samples analyzed and the sample implanted in mice in most cases were from different parts of the tumor. Although the xenograft profiles were very similar to their sample of origin (Fig. 1), there were moderate numbers of changes after transplantation (Table 2, Fig. 3A). From the individual tumor profiles (Fig. 2), it seems that many of the changes appear as shifts of entire chromosome profiles, which suggests they are caused by chromosomal aneuploidy and clonal drift or selection. We do not expect this to cause a systematic bias; and, when comparing the frequency of the different changes in patient-xenografts pairs, only 1 change toward more gain or loss appeared in more than 1 sample (increased loss of 16q23.2-23.3 in 2 osteosarcoma pairs) (Fig. 3A). Although this may have been caused by a selection process, the observation of 2 such changes in 4 sample pairs was not significant.

Another issue is the changes that may appear in the xenografts during passaging over time. The xenotransplanted tumor would be expected to evolve over time, as would the patient tumor. Possible model-specific differences would be the absence of a strong selection for immune evasion, the repeated subsampling bias during each passage, and the continuous selection for growth in the mouse model, which could provide atypical selection pressures. In addition, the reduced interactions between cancer cells and the host stroma because of species differences could affect the selection pressures experienced by the cancer cells. Conversely, because all of these patients receive presurgical chemotherapy, cells in the surgical specimen that survive and are able to initiate new tumors may be selected for properties that provide resistance to chemotherapy, which subsequently are not selected for and may be lost.

The heat map in Figure 3B illustrates the differences between early and late passages of the various xenografts. The heat map also indicates that changes toward more normal profiles were most common: Increased losses were more frequent than increased gains, and, in general, the pattern was scattered. It is striking that the 2 only segments gained in any pair were on each arm of chromosome 4 and were gained in 2 of 6 samples each. Because there were so few changes toward increased gains, finding 2 such changes for the same segment was significant, even after correcting for multiple testing. However, given the low number of samples, even significant changes should be treated with some caution until confirmed by other means. Both regions were approximately 2 Mb and contained numerous genes, several of which are cancer-associated.

In the 4p region, the paired-like homeobox 2b protein (PHOX2B) is involved in the development of v-myc myelocytomastosis viral oncogene homolog (MYC)-driven neuroblastomas[27]; PDS5 regulator of cohesion maintenance homolog A (*PDS5A*) is involved in proliferation[28]; LIM and calponin homology domains 1 (*LIMCH1*) codes for a modulator of Notch/Wnt in mesoderm development[28,29]; and ras homolog gene family, member H (RhoH) regulates migration, proliferation, survival, and engraftment of hematopoietic cells.[30,31] In 4q, several genes reportedly are amplified in nervous system tumors,[32] and both amplicons were observed in approximately 25% of our EuroBoNeT panel of

osteosarcoma patient samples (Kuijjer et al, unpublished data); thus, this amplicon does not appear to be a model-specific artifact but, rather, is a sign of tumor progression. The most likely candidate in this region appears to be *PDGFRA*, which also is implicated in the oncogenesis of osteosarcoma and can be exploited as a therapeutic target.[33-36] In addition to being amplified in glioblastomas,[32] it has been observed that *CHIC2* is fused to ets variant 6 (*ETV6*) in some leukemias.[37] *FIP1L1* can be fused to *PDGFRA* in eosiniphilic leukemias, and the fusion gene induces this lineage in hematopoietic stem cells.[38,39] *LNX1* codes for a numb ligand, which may be down-regulated in gliomas[32,40,41]; *RASL11B* is a member of the *ras* family of oncogenes with unknown function[32]; and *SCFD2* appears to be involved in the DNA damage response and is regulated by p53.[42]

The gains in region 21q22.3-qtel that were lost during passaging in 5 of 6 osteosarcoma samples (Fig. 3B) would be expected to contain genes that were selected for in the patient but for which the selection pressure disappeared in the mouse. Several such possible candidate genes were identified in this 4.5-Mb region, including autoimmune regulator (*AIRE*), which is involved in immune tolerance[43]; β2-intergin (*ITGB2*) (CD18), which is involved in tumor macrophage recruitment and vascularization[44]; and inducible T-cell costimulator ligand (*ICOSLG*), which is involved in tumor-mediated immune suppression.[45,46] Another possibility, however, is that this amplification was caused by the chemotherapy the patient received, because the region contained adenosine triphosphate (ATP)-binding cassette subfamily G (WHITE) member 1 (*ABCG1*), which codes for a classic drug efflux pump; chromosome 21 open reading frame 56 (*C21orf56*), which reportedly provides resistance to alkylating agents[47]; and formiminotransferase cyclodeaminase (*FTCD*)[48] and solute carrier family 19 (folate transporter) member 1 (*SLC19A1*) (also called FOLT, RFC1, IFC1[49,50]), which are involved in folate metabolism and the transport of methotrexate, respectively.

Little is known about the genes in 22q13 that were (partially) lost in the early passage but reappeared in the late passage of 3 of 6 osteosarcoma xenografts ($P = .0027$), except for cermide kinase (*CERK*) and family with sequence similarity 19 (chemokine [C-C motif]-like) member A5 (*FAM19A5*) (also called *TAFA5*), which also seem to be involved in immune cell function and host stroma interactions.[51,52] Germ-line copy number variations and aberrations in tumors with *TAFA5* also have been implicated in the development of glioblastoma multiforme and the sarcoma subtype malignant peripheral nerve sheath tumors (formerly malignant schwannomas).[51,53] It seems plausible that aberrations of any of these genes may contribute to immune evasion in the patient but may not be required in an immune-compromised host.

Tumors obviously evolve over time, whether in the patient or during growth in mice. Many of the scattered copy number changes are frequent in osteosarcoma patient samples,[54] and we would expect them to represent normal tumor progression rather than transplantation-specific artifacts. An interesting illustration of this aspect was the study by Ding et al,[55] who used full genome sequencing to identify clear differences between a primary tumor and its derived xenograft. However, most of these differences were maintained in a later brain metastasis, indicating that the metastatic cells were present in the primary tumor and were the cells that could successfully establish new tumors both in the mice and at the remote site in the patient.

In other studies (Namlos et al and Kresse et al, unpublished data), we will characterize our osteosarcoma xenograft panel with regard to messenger RNA and microRNA expression profiles as well as promoter methylation patterns. The biologic properties of the cell lines and xenografts, eg, with regard to vascularization, growth pattern, tumorigenicity, metastasis, etc, are being characterized by other members of our consortium and will be published later.

We conclude that these xenograft models reflect the patient tumors well and are of high value as preclinical disease models. The significant artifacts observed appear to relate to selection pressures that are present in the patient but not in the mice. When these phenomena are taken into consideration, the models should be applicable to most kinds of therapeutic studies that do not require an efficient host immune system.

FUNDING SOURCES

This work was supported by the European Network to Promote Research into Uncommon Cancers in Adults and Children: Pathology, Biology, and Genetics of Bone Tumors (contract 018814 from the European Community Sixth Framework Program; see http://www.eurobonet.eu; accessed January 2011); the University of Oslo; the Norwegian Cancer Society; and the Functional Genomics Programme (FUGE) of the Research Council of Norway. The genomic microarrays were provided by the Norwegian Microarray Consortium at the National Technology Platform, and the statistical analysis was done by the Bioinformatics platform, both supported by the FUGE of the Research Council of Norway.

CONFLICT OF INTEREST DISCLOSURES

The authors made no disclosures.

REFERENCES

1. Morton CL, Houghton PJ. Establishment of human tumor xenografts in immunodeficient mice. *Nat Protoc*. 2007; 2:247-250.
2. Marangoni E, Vincent-Salomon A, Auger N, et al. A new model of patient tumor-derived breast cancer xenografts for preclinical assays. *Clin Cancer Res*. 2007;13:3989-3998.
3. Fiebig H, Maier A, Burger A. Clonogenic assay with established human tumour xenografts: correlation of in vitro to in vivo activity as a basis for anticancer drug discovery. *Eur J Cancer*. 2004;40:802-820.
4. Garber K. From human to mouse and back: "tumorgraft" models surge in popularity. *J Natl Cancer Inst*. 2009;101: 6-8.
5. Kerbel RS. Human tumor xenografts as predictive preclinical models for anticancer drug activity in humans: better than commonly perceived-but they can be improved. *Cancer Biol Ther*. 2003;2(4 suppl 1):S134-S139.
6. Guenot D, Guerin E, Aguillon-Romain S, et al. Primary tumour genetic alterations and intra-tumoral heterogeneity are maintained in xenografts of human colon cancers showing chromosome instability. *J Pathol*. 2006;208:643-652.
7. Voskoglou-Nomikos T, Pater JL, Seymour L. Clinical predictive value of the in vitro cell line, human xenograft, and mouse allograft preclinical cancer models. *Clin Cancer Res*. 2003;9:4227-4239.
8. Lydiatt WM, Murty VV, Davidson BJ, et al. Homozygous deletions and loss of expression of the CDKN2 gene occur frequently in head and neck squamous cell carcinoma cell lines but infrequently in primary tumors. *Genes Chromosomes Cancer*. 1995;13:94-98.
9. Daniel VC, Marchionni L, Hierman JS, et al. A primary xenograft model of small-cell lung cancer reveals irreversible changes in gene expression imposed by culture in vitro. *Cancer Res*. 2009;69:3364-3373.
10. Whiteford CC, Bilke S, Greer BT, et al. Credentialing preclinical pediatric xenograft models using gene expression and tissue microarray analysis. *Cancer Res*. 2007;67:32-40.
11. Francis P, Namlos HM, Muller C, et al. Diagnostic and prognostic gene expression signatures in 177 soft tissue sarcomas: hypoxia-induced transcription profile signifies metastatic potential [serial online]. *BMC Genomics*. 2007; 8:73.
12. Helman LJ, Meltzer P. Mechanisms of sarcoma development. *Nat Rev Cancer*. 2003;3:685-694.
13. Ottaviano L, Schaefer K, Gajewski M, et al. Molecular characterization of commonly used cell lines for bone tumor research: a trans-European EuroBoNet effort. *Genes Chromosomes Cancer*. 2010;49:40-51.
14. Fletcher CDM, Unni KK, Mertens F, eds. Pathology and Genetics of Tumours of Soft Tissue and Bone. World Health Organization Classification of Tumours. Lyon, France: IARC Press; 2002.
15. Bruheim S, Bruland OS, Breistol K, Maelandsmo GM, Fodstad O. Human osteosarcoma xenografts and their sensitivity to chemotherapy. *Pathol Oncol Res*. 2004;10:133-141.
16. Meza-Zepeda LA, Kresse SH, Barragan-Polania AH, et al. Array comparative genomic hybridization reveals distinct DNA copy number differences between gastrointestinal stromal tumors and leiomyosarcomas. *Cancer Res*. 2006; 66:8984-8993.
17. Wang J, Meza-Zepeda LA, Kresse SH, Myklebost O. M-CGH: analysing microarray-based CGH experiments [serial online]. *BMC Bioinformatics*. 2004;5:74.
18. Tusher VG, Tibshirani R, Chu G. Significance analysis of microarrays applied to the ionizing radiation response. *Proc Natl Acad Sci U S A*. 2001;98:5116-5121.
19. Dysvik B, Jonassen I. J-Express: exploring gene expression data using Java. *Bioinformatics*. 2001;17:369-370.
20. Olshen AB, Venkatraman ES, Lucito R, Wigler M. Circular binary segmentation for the analysis of array-based DNA copy number data. *Biostatistics*. 2004;5:557-572.
21. Benjamini Y, Hochberg Y. Controlling the false discovery rate: a practical and powerful approach to multiple testing. *J R Stat Soc B*. 1995;57:289-300.
22. Mayordomo E, Machado I, Giner F, et al. A tissue microarray study of osteosarcoma: histopathological and immunohistochemical validation of xenotransplanted tumors as preclinical models. *Appl Immunohistochem Mol Morphol*. 2010;18:453-461.
23. Shoemaker RH. The NCI60 human tumour cell line anticancer drug screen. *Nat Rev Cancer*. 2006;6:813-823.
24. Neale G, Su X, Morton CL, et al. Molecular characterization of the pediatric preclinical testing panel. *Clin Cancer Res*. 2008;14:4572-4583.
25. Jeuken JW, Sprenger SH, Wesseling P, et al. Genetic reflection of glioblastoma biopsy material in xenografts: characterization of 11 glioblastoma xenograft lines by comparative genomic hybridization. *J Neurosurg*. 2000;92:652-658.
26. Francis P, Fernebro J, Eden P, et al. Intratumor versus intertumor heterogeneity in gene expression profiles of soft-tissue sarcomas. *Genes Chromosomes Cancer*. 2005;43:302-308.
27. Alam G, Cui H, Shi H, et al. MYCN promotes the expansion of Phox2B-positive neuronal progenitors to drive neuroblastoma development. *Am J Pathol*. 2009;175:856-866.
28. Zheng MZ, Zheng LM, Zeng YX. SCC-112 gene is involved in tumor progression and promotes the cell proliferation in G2/M phase. *J Cancer Res Clin Oncol*. 2008; 134:453-462.
29. Sewell W, Sparrow DB, Smith AJ, et al. Cyclical expression of the Notch/Wnt regulator Nrarp requires modulation by Dll3 in somitogenesis. *Dev Biol*. 2009;329:400-409.
30. Gu Y, Jasti AC, Jansen M, Siefring JE. RhoH, a hematopoietic-specific Rho GTPase, regulates proliferation, survival, migration, and engraftment of hematopoietic progenitor cells. *Blood*. 2005;105:1467-1475.
31. Chae HD, Lee KE, Williams DA, Gu Y. Cross-talk between RhoH and Rac1 in regulation of actin cytoskeleton and chemotaxis of hematopoietic progenitor cells. *Blood*. 2008; 111:2597-2605.
32. Holtkamp N, Ziegenhagen N, Malzer E, Hartmann C, Giese A, von Deimling A. Characterization of the amplicon on chromosomal segment 4q12 in glioblastoma multiforme. *Neuro Oncol*. 2007;9:291-297.
33. Corless CL, Heinrich MC. Molecular pathobiology of gastrointestinal stromal sarcomas. *Annu Rev Pathol*. 2008;3:557-586.

34. McGary EC, Weber K, Mills L, et al. Inhibition of platelet-derived growth factor-mediated proliferation of osteosarcoma cells by the novel tyrosine kinase inhibitor STI571. *Clin Cancer Res*. 2002;8:3584-3591.
35. Sulzbacher I, Birner P, Trieb K, Traxler M, Lang S, Chott A. Expression of platelet-derived growth factor-AA is associated with tumor progression in osteosarcoma. *Mod Pathol*. 2003;16:66-71.
36. Kubo T, Piperdi S, Rosenblum J, et al. Platelet-derived growth factor receptor as a prognostic marker and a therapeutic target for imatinib mesylate therapy in osteosarcoma. *Cancer*. 2008;112:2119-2129.
37. Kuchenbauer F, Schoch C, Holler E, Haferlach T, Hiddemann W, Schnittger S. A rare case of acute myeloid leukemia with a CHIC2-ETV6 fusiongen and multiple other molecular aberrations. *Leukemia*. 2005;19:2366-2368.
38. Valent P. Pathogenesis, classification, and therapy of eosinophilia and eosinophil disorders. *Blood Rev*. 2009;23:157-165.
39. Fukushima K, Matsumura I, Ezoe S, et al. FIP1L1-PDGFRalpha imposes eosinophil lineage commitment on hematopoietic stem/progenitor cells. *J Biol Chem*. 2009; 284:7719-7732.
40. Chen J, Xu J, Zhao W, et al. Characterization of human LNX, a novel ligand of Numb protein X that is downregulated in human gliomas. *Int J Biochem Cell Biol*. 2005;37:2273-2283.
41. Blom T, Roselli A, Tanner M, Nupponen NN. Mutation and copy number analysis of LNX1 and Numbl in nervous system tumors. *Cancer Genet Cytogenet*. 2008;186:103-109.
42. Krieg AJ, Hammond EM, Giaccia AJ. Functional analysis of p53 binding under differential stresses. *Mol Cell Biol*. 2006;26:7030-7045.
43. Abramson J, Giraud M, Benoist C, Mathis D. Aire's partners in the molecular control of immunological tolerance. *Cell*. 2010;140:123-135.
44. Qualls JE, Murray PJ. A double agent in cancer: stopping macrophages wounds tumors. *Nat Med*. 2010;16:863-864.
45. Schreiner B, Wischhusen J, Mitsdoerffer M, et al. Expression of the B7-related molecule ICOSL by human glioma cells in vitro and in vivo. *Glia*. 2003;44:296-301.
46. Strauss L, Bergmann C, Szczepanski MJ, Lang S, Kirkwood JM, Whiteside TL. Expression of ICOS on human melanoma-infiltrating CD4+CD25highFoxp3+ T regulatory cells: implications and impact on tumor-mediated immune suppression. *J Immunol*. 2008;180:2967-2980.
47. Fry RC, Svensson JP, Valiathan C, et al. Genomic predictors of interindividual differences in response to DNA damaging agents. *Genes Dev*. 2008;22:2621-2626.
48. Hilton JF, Christensen KE, Watkins D, et al. The molecular basis of glutamate formiminotransferase deficiency. *Hum Mutat*. 2003;22:67-73.
49. Wong SC, Proefke SA, Bhushan A, Matherly LH. Isolation of human cDNAs that restore methotrexate sensitivity and reduced folate carrier activity in methotrexate transport-defective Chinese hamster ovary cells. *J Biol Chem*. 1995; 270:17468-17475.
50. Williams FM, Flintoff WF. Isolation of a human cDNA that complements a mutant hamster cell defective in methotrexate uptake. *J Biol Chem*. 1995;270:2987-2992.
51. Diaz de Stahl T, Hartmann C, de Bustos C, et al. Chromosome 22 tiling-path array-CGH analysis identifies germ-line- and tumor-specific aberrations in patients with glioblastoma multiforme. *Genes Chromosomes Cancer*. 2005; 44:161-169.
52. Arana L, Gangoiti P, Ouro A, Trueba M, Gomez-Munoz A. Ceramide and ceramide 1-phosphate in health and disease [serial online]. *Lipids Health Dis*. 2010;9:15.
53. Diaz de Stahl T, Hansson CM, de Bustos C, et al. High-resolution array-CGH profiling of germline and tumor-specific copy number alterations on chromosome 22 in patients affected with schwannomas. *Hum Genet*. 2005;118:35-44.
54. Kresse SH, Ohnstad HO, Paulsen EB, Bjerkehagen B, Myklebost O, Meza-Zepeda LA. LSAMP, a novel candidate tumor suppressor gene in human osteosarcomas identified by array CGH. *Genes Chromosomes Cancer*. 2009;48:679-693.
55. Ding L, Ellis MJ, Li S, et al. Genome remodelling in a basal-like breast cancer metastasis and xenograft. *Nature*. 2010;464:999-1005.